Integrated quantum optical networks based on quantum dots and photonic crystals

New Journal of Physics

Integrated quantum optical networks based on quantum dots and photonic crystals

Andrei Faraon[1,4]**, Arka Majumdar**[2]**, Dirk Englund**[3]**, Erik Kim**[2]**, Michal Bajcsy**[2] **and Jelena Vučković**[2]

[1] Hewlett-Packard Laboratories, 1501 Page Mill Road, Palo Alto, CA 94304, USA
[2] E L Ginzton Laboratory, Stanford University, Stanford, CA 94305, USA
[3] Department of Electrical Engineering and Department of Applied Physics, Columbia University, New York, NY 10027, USA
E-mail: andrei.faraon@hp.com

Abstract. Single solid-state optical emitters have quantum mechanical properties that make them suitable for applications in information processing and sensing. Most of these quantum technologies rely on the capability to integrate the emitters in reliable solid-state optical networks. In this paper, we present integrated devices based on GaAs photonic crystals and InAs self-assembled quantum dots. These quantum networks are well suited to future optoelectronic devices operating at ultralow power levels, single-photon logic devices and quantum information processing.

Contents

[4] Author to whom any correspondence should be addressed.

1. Introduction

Nano-photonic devices based on quantum optical effects at the single-emitter and single-photon level represent a fundamental technological limit for the on-chip processing of classical and quantum information [1, 2]. The basic building blocks of these devices are single optical quantum emitters integrated in a micro/nano-photonic network. One of the emitters that is most suitable for integration is the InAs quantum dot in GaAs because of its excellent optical properties and the well-developed GaAs semiconductor fabrication techniques [3]. In some applications, quantum dots (QDs) coupled to nano-scale optical resonators can be used as simple optical dipoles that can act as efficient light switches or highly nonlinear optical media [4]. For quantum information applications, it is essential to use emitters whose quantum state can be optically controlled. With InAs QDs, quantum information can be encoded in the electron or hole spin that can be completely manipulated using fast optical pulses [5, 6].

The nano-photonic platform consists of devices that provide strong localization of the electro-magnetic field, all interconnected in an optical network. Strong localization is essential for enhancing the interaction strength between the photons and the QDs. Micro- and nano-scale resonators, such as micro-pillars, microdiscs, micro-rings and photonic crystal cavities, represent viable resonator choices depending on the particular application [7]. The advantage of using photonic crystal cavities is that they have extremely small optical mode volumes and are well suited to integration with optical waveguides and on-chip electronics [8, 9].

In this paper, we discuss our recent progress in building integrated photonic crystal quantum networks with coupled QDs. One immediate goal is to be able to fabricate reliable integrated devices for optoelectronic applications where QDs coupled to resonators act as optical switches. Once this goal is achieved, the next step is to perform optical spin control of individual QDs in a network for quantum computing applications.

2. Single quantum dots (QDs) coupled to photonic crystal cavities

For the optical quantum networks discussed in this paper, the basic building block consists of a photonic crystal cavity coupled to a single QD. The quantum optics properties of this quantum system enable energy-efficient optical switches, ultrahigh optical nonlinearities and quantum information devices.

The InAs QDs used in our experiments are three-dimensional (3D) islands of InAs embedded in GaAs, and are grown by molecular beam epitaxy on GaAs wafers, as described in [3]. Due to the bandgap difference between GaAs (1.42 eV) and InAs (0.35 eV), and the effects of strain, these QDs form an effective 3D potential well that serves as a trapping potential for electrons and holes. The tight spatial confinement causes the energy levels of the QD to be discrete, so the QDs can exhibit atom-like properties. InAs QDs can be designed to operate at various wavelengths spanning the entire near-infrared spectrum. For applications in quantum information science, it is desirable to operate below the wavelength of $1\,\mu$m because of the high-performance silicon photodetectors available in this wavelength range. For optical signal processing, it is advantageous to use QDs that operate closer to the telecom wavelength, because of the lower GaAs optical loss in this spectral region and the deeper confinement of the exciton. We use QDs operating around 940 nm, with a bulk lifetime of a few nanoseconds and near-unity quantum efficiency. The QD density in the devices discussed in this paper is $\approx 100\,\mu$m^{-2}.

One of the most widely used resonators for integration in photonic crystal optical networks is the linear three-hole defect cavity [10]. It is made by omitting three holes in a row in a triangular photonic crystal lattice. This cavity does not have the smallest possible optical mode volume or the highest quality factor. However, it provides a very good compromise between small mode volume (close to one cubic wavelength), high quality factor (theoretical value exceeding 10^5 not yet reached in experiments with QDs), large enough physical volume to relieve the challenge of spatial overlap with QDs and robustness against fabrication imperfections (the quality factor and wavelength are tolerant to defects due to fabrication), when compared with other photonic crystal resonators. The photonic crystal devices presented in this paper were fabricated in a 160 nm thick GaAs membrane. This membrane was grown via molecular beam epitaxy (MBE) on top of a 1 μm thick AlGaAs sacrificial layer sitting on the GaAs substrate. A layer of QDs was embedded in the middle of the membrane during the growth process.

The physics of the cavity–QD coupled system is usually described using the Jaynes–Cummings Hamiltonian, given by the equation

$$\hat{H} = \frac{\hbar\omega_{QD}}{2}\hat{\sigma}_z + \hbar\omega_c\left(\hat{a}^\dagger\hat{a} + \frac{1}{2}\right) + i\hbar(g^*\hat{a}^\dagger\hat{\sigma}_- - g\hat{\sigma}_+\hat{a}), \tag{1}$$

where ω_{QD} (ω_c) is the resonance frequency of the QD (cavity), g is the coupling constant between the field and the dipole, a and $a^\dagger$ are the annihilation and creation operators for the cavity field, $\sigma_- = |g\rangle\langle e|$ and $\sigma_+ = |e\rangle\langle g|$ are the rising and lowering operators for the atom ($|g\rangle$ and $|e\rangle$ are the ground and excited states of the atom) and $\sigma_z = |e\rangle\langle e| - |g\rangle\langle g|$ is the population operator. After adding damping from the cavity field decay rate κ and dipole free space decay rate γ, the eigenstates of this Hamiltonian are

$$\omega_\pm = \frac{\omega_c + \omega_{QD}}{2} - i\frac{\kappa + \gamma}{2} \pm \sqrt{g^2 + \frac{1}{4}(\delta - i(\kappa - \gamma))^2}, \tag{2}$$

where $\delta = \omega_{QD} - \omega_c$ is the QD/cavity detuning. For $\delta = 0$ and $\kappa \gg \gamma$, the real part of the system eigenstates are degenerate for $g < \kappa/2$ (weak coupling regime) and non-degenerate with splitting $\sim 2g$ for $g > \kappa/2$ (strong coupling regime) [11, 12].

Under weak coherent excitation, the transmission function of an optical resonator with a coupled QD is given by

$$T = \eta\left|\frac{\kappa}{i(\omega_c - \omega) + \kappa + \frac{g^2}{i(\omega_{QD} - \omega) + \gamma}}\right|^2, \tag{3}$$

where ω is the probe frequency, and η is a scaling factor that depends on the coupling efficiency into the cavity.

For typical parameters found experimentally in GaAs photonic crystal cavities coupled to InAs QDs ($\kappa/2\pi = 16$ GHz, $\gamma/2\pi \sim 0.1$ GHz), the normalized transmission function is shown in figure 1. What makes this system remarkable is that the presence of the coupled dipole can change the system from fully transparent to opaque even for modest values of the coupling rate g when the system is not in the strong coupling regime [13]. This simple property is essential for implementing quantum repeaters for quantum information processing [13], or basic optoelectronic switches that operate at ultralow energy levels. For switching applications, the frequency of the quantum emitter can be controlled using external factors as local electric fields [14] or even other optical fields [15].
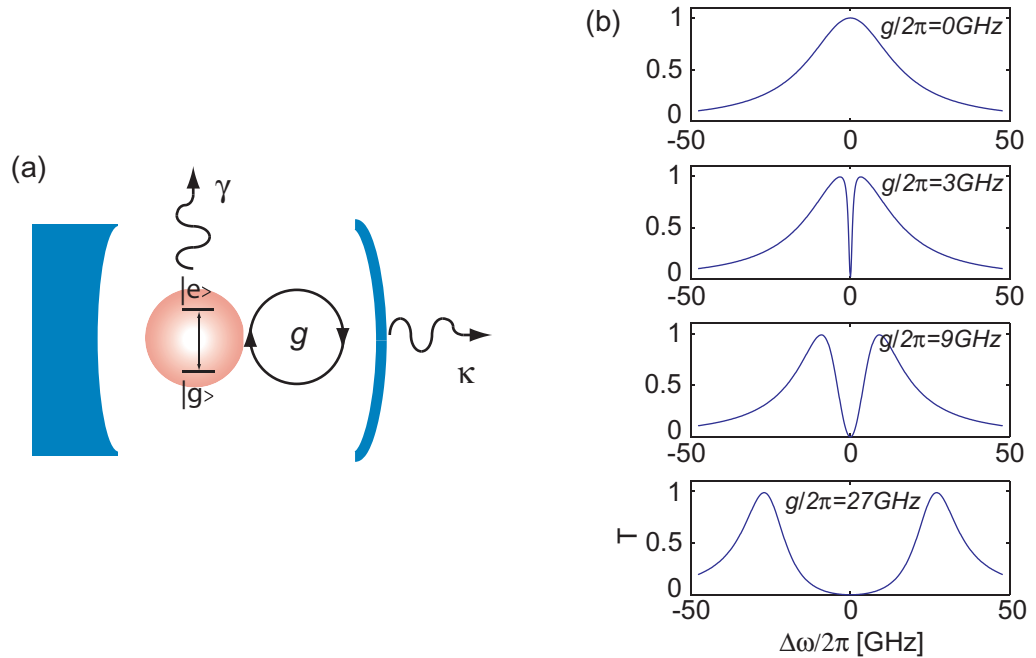
Figure 1. (a) Schematic representation of a one-sided optical cavity with a coupled optical dipole. The dipole couples to the cavity mode with rate g, the cavity field decay rate is κ and the spontaneous emission rate of the atom is γ. (b) Theoretical transmission spectra of a coupled cavity/quantum dot system ($\kappa/2\pi = 16\,\text{GHz}$, $\gamma/2\pi = 0.1\,\text{GHz}$) for different values of the coupling constant g. These spectra indicate that the transmission function of the cavity is significantly affected by the presence of the dipole, even in the weak coupling regime ($g < \kappa/2$).

Another remarkable property of the cavity–QD system is that it exhibits optical nonlinearities at the single photon level. The cause of these nonlinearities is the anharmonic ladder of energy eigenstates of a strongly coupled system (equation (1)). When the QD and the cavity are in resonance, the energy eigenstates are grouped into two-level manifolds denoted by $|n, \pm\rangle$, with energies $\hbar\omega_{n,\pm} = \hbar(n\omega_\text{c} \pm g\sqrt{n})$, where n is the number of energy quanta in the system and ω_c is the bare cavity frequency (figure 2). Interesting single-photon phenomena appear just by considering the first two excited level manifolds. For example, the energy difference between $|0\rangle$ and $|1, -\rangle$ is $\hbar(\omega_\text{c} - g)$, while that between $|1, -\rangle$ and $|2, -\rangle$ is $\hbar(\omega_\text{c} - g(\sqrt{2} - 1))$. This implies that only one photon with energy $\hbar(\omega_\text{c} - g)$ can be coupled at a time into the system because there are no available energy eigenstates at $2 \times \hbar(\omega_\text{c} - g)$, a phenomenon known as photon blockade [16–18]. At the same time, a photon with energy $\hbar(\omega_\text{c} - g(\sqrt{2} - 1))$ cannot be coupled if the system is in the ground state, but this becomes possible if accompanied by another photon with energy $\hbar(\omega_\text{c} - g)$.

These single-photon nonlinearities open up the possibility of using the system for single-photon logic devices. However, in order for these to be effective, it is necessary that the optical width of the system resonances (limited by the decay rate of the cavity and the QD) is significantly smaller than their separation. With current state of the art devices, the separation is of the order of the linewidth.
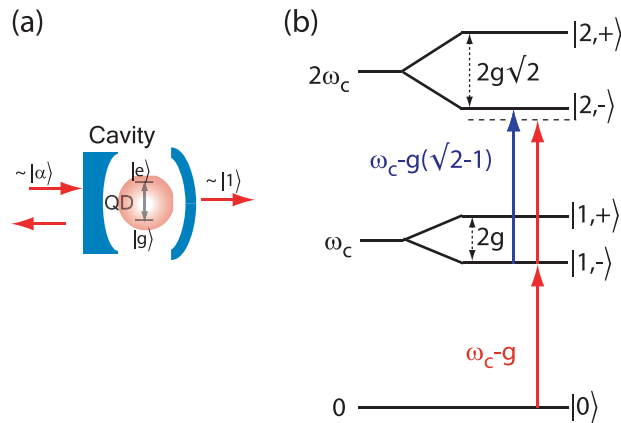
Figure 2. (a) Schematic representation of an optical cavity strongly coupled to a single quantum emitter. In photon blockade operation, a coherent state is incident on one side of the cavity and single-photon states exit at the other side. (b) Diagram showing the anharmonic ladder of energy eigenstates of a strongly coupled system.
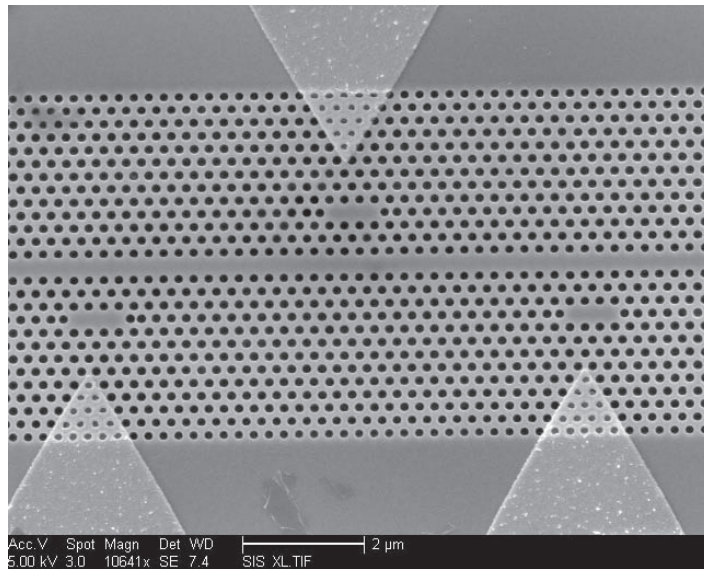

Figure 3. The photonic crystal network device consisting of three resonators coupled to a common waveguide. Metal electrodes are deposited in close proximity to the cavities for electrical control.

3. On-chip integration

To take advantage of the quantum optical properties of single emitters coupled to nano-resonators, these systems need to be connected into an on-chip optical network for information processing [19]. These networks should integrate optical resonators with coupled emitters interconnected via optical waveguides (figure 3). One of the main difficulties in implementing these devices comes from the spectral inhomogeneous broadening and the random location
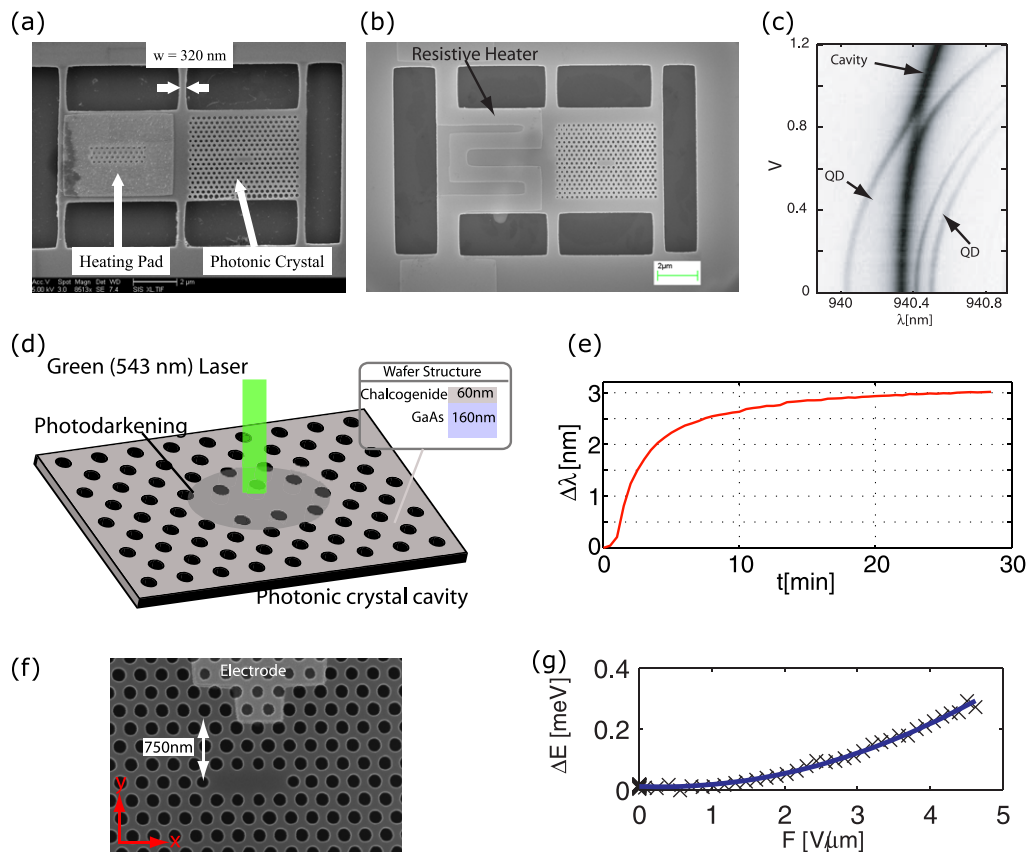
Figure 4. (a) Device for local temperature tuning using laser heating. The heating laser is focused on a metal-coated heating pad that absorbs light above the GaAs bandgap. (b) Photonic crystal device equipped with a resistive heater to control its temperature. (c) Tuning the cavity and QDs using the resistive heater. (d) Principle of local tuning using chalcogenide glasses. A green laser focused on the cavity causes the refractive index of the glass to increase, thus red-shifting the cavity resonance. (e) Tuning the cavity resonance using a 60 nm layer of chalcogenide glass (As_2S_3). (f) Photonic crystal cavity and metallic electrode for fast, local QD tuning using laterally applied electric fields. (g) QD tuning using the dc Stark effect.

that characterizes most solid-state emitters in bulk material. In the case of InAs QDs, these are caused by the randomness associated with the molecular beam epitaxy self-assembly process. Currently, there are growth techniques under development for site-controlled QDs that promise to solve the problem of random spatial location [20]. However, the spectral properties of these QDs still need to be improved for quantum optics experiments. Currently, there is not an imminent material science solution for the spectral inhomogeneous broadening, so the community is relying on local tuning techniques [14], [21–25].

We developed three local tuning techniques that allow for independent control of the cavity and QD frequency (figure 4). The first technique relies on local control of the temperature, which can be implemented by locally heating the area on the chip next to the QD of interest. We have implemented this technique using both an external laser beam for local heating (figure 4(a)) [21]

and lithographically defined resistive heaters (figure 4(b)) [23]. The semiconductor bandgap and the index of refraction are sensitive to temperature, which causes both the QD and the cavity resonance to be temperature dependent. The temperature tuning of a QD into resonance with a cavity is shown in figure 4(c). In this case, the tuning was done by changing the voltage across the resistive heater in figure 4(b). The system operates in the strong coupling regime, as indicated by the anti-crossing of the spectral lines. Compared with the cavity, the QD red-shifts roughly three times faster as the temperature is increased from 4 to 50 K. This implies that temperature tuning by itself cannot be used to fully align the cavities and QDs in a network. More flexibility can be achieved by combining this technique with one based on photorefractive materials deposited on the surface of the chip. We have used a thin layer (under 100 nm) of As_2S_3 deposited on the membrane that changes its index of refraction under green excitation, thus causing the cavity resonance to red-shift (figure 4(d)). We have observed shifts of up to 3 nm with cavities operating at 930 nm as shown in figure 4(e) [22]. In principle, this technique can be used to affect only the cavity resonance, and could provide complete tuning capabilities when combined with temperature tuning. Another method for local tuning of QDs is to use dc electric fields applied via electrodes deposited in close proximity to the cavity/QD system of interest (figure 4(f)) [14]. In this case, when a bias voltage is applied to the metallic electrode, a depletion region, and thus an electric field, is created. The electric field causes the QD to red-shift via the quantum confined Stark effect. The shift in the QD resonance with electric field is shown in figure 4(g). The value of the electric field is not measured but inferred from the value of the bias voltage and the geometry of the device.

These types of tuning techniques will most probably find their place in future on-chip quantum networks, regardless of the particular material system. All of the solid-state quantum emitters and resonators are sensitive to local perturbations in the solid-state environment (i.e. strain, local charge accumulation and imperfections in the fabrication process), so some type of local tuning will need to be employed.

In terms of integration, some of the most complex devices that have been realized still employ a single quantum emitter [26]. One of these devices is shown in figure 5(a), and it consists of a photonic crystal cavity coupled to a waveguide that is terminated with a grating outcoupler. The device is built in a suspended membrane that is connected with the rest of the substrate using only a few narrow bridges that ensure the device thermal insulation. The temperature of the device is controlled using an external laser beam focused on the metal pad. The transmission function of the device is characterized using a laser beam coupled from the top into the cavity. The light then couples into the waveguide and the output scattered from the grating is collected using the same confocal microscope setup as used for light injection. The measurement is made by fixing constant the frequency of the probe laser, and by tuning the cavity and QD resonance using the local temperature control (see [4] for more details). The transmission function of the system is shown in figure 5(b). The drop in the transmission function is caused by the coherent interaction among the probe laser field, cavity field and the coupled QD. The QD is in the weak coupling regime, as indicated by the fit (equation (3)) using parameters $g/2\pi = 9.4$ GHz, $\kappa/2\pi = 33$ GHz and $\gamma/2\pi = 0.3$ GHz. This type of device can be directly used to implement photonic modules for efficient generation of entangled photon states [27]. The photonic modules use a single atomic/QD qubit to mediate the generation of entanglement between subsequent photons that form a cluster state for quantum computing.

One application of these basic quantum networks is for electro-optic modulation using a single QD [28]. This has already been demonstrated using just a single photonic crystal cavity
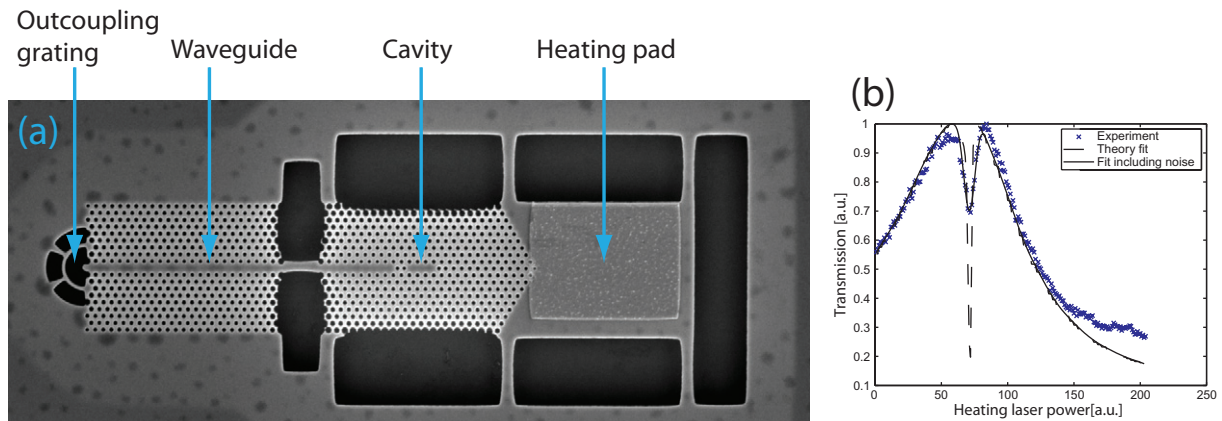
Figure 5. (a) The photonic crystal device integrating a cavity coupled to a waveguide that is terminated with a grating for efficient light scattering. An external laser beam focused directly on the metal heating pad on the left is used to locally control the temperature of the device that is correlated with the cavity and QD wavelength. (b) Transmission measurement showing the Lorentzian spectrum and the drop in transmission caused by the coherent interaction with the QD.

with a strongly coupled QD, which was probed using a reflectivity measurement [14]. The frequency of the QD was controlled using a bias electric field applied using a metallic Schottky electrode. This type of electro-optic switch operates at the fundamental level of light–matter interaction, where the transmission function is controlled using single quantum emitters at the level of a few photons per characteristic lifetime of the system. This type of device can operate at speeds up to 10 GHz, can handle light intensities up to 10 nW, and can be switched using energies less than 1 fJ. In order to use this single QD electro-optic modulator for on-chip optical signal processing, it is necessary to integrate it in a photonic network. A concept device of this type is shown in figure 6. In this case, the cavity is butt-coupled to two photonic crystal waveguides that serve as the input and output ports.

Electrical control of the cavity–QD system can also be achieved by applying an electric field parallel to the growth (vertical with respect to the wafer plane) direction. This can be implemented using a p–i–n junction embedded in the photonic crystal membrane during the MBE process [29]. As the vertical confinement in a QD is stronger than the lateral confinement, the induced Stark shift is higher in this configuration. Also, in the vertical direction the QD has a large permanent dipole moment, and hence the quantum confined Stark shift is primarily linear, in contrast to quadratic, as we observed in the lateral electrical control.

The fabrication process for devices with vertical electrical control is shown in figure 7. Metal electrodes are deposited to make contact with the n-GaAs and p-GaAs layers. First, an etching step using sulfuric acid and hydrogen peroxide is used to expose the n-GaAs layer. Separate lithography steps are then used to deposit p- and n-contacts because the n-contact and p-contact are made of different materials. The photonic crystal devices are fabricated after depositing the contacts.

The optical system is probed both resonantly using the reflectivity method [4] and by using photoluminescence. The reflectivity obtained from the cavity is shown in figure 8(a) for two
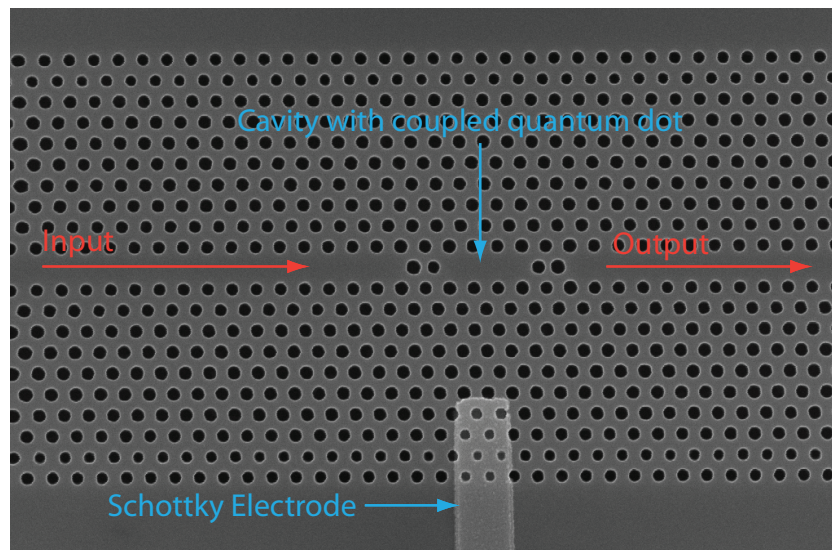
Figure 6. Integrated electro-optic switch (concept device) for on-chip optical signal processing. The transmission function is controlled using a single QD coupled to the cavity. The QD frequency can be changed using a bias electric field applied via a Schottky electrode.
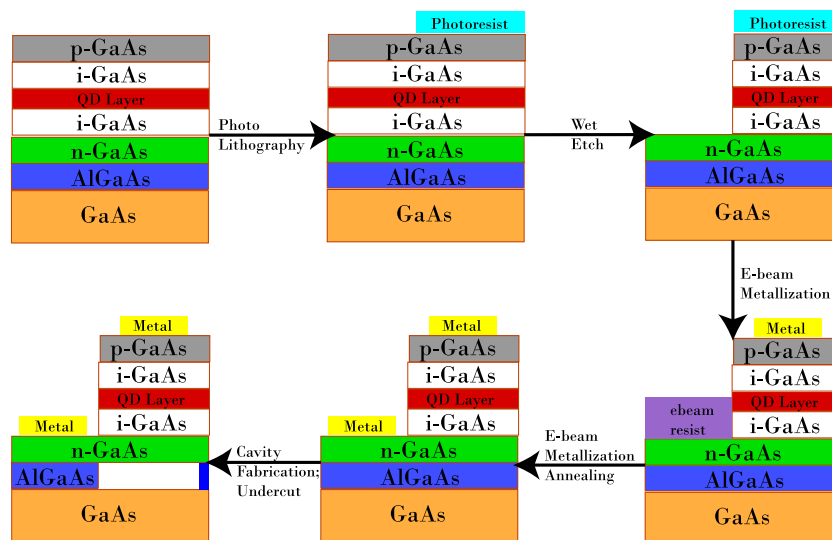

Figure 7. Fabrication steps for contacts and photonic crystal devices enabling electrical control in a p–i–n junction. Here, p-GaAs, n-GaAs and i-GaAs indicate p-doped, n-doped and intrinsic gallium arsenide, respectively.

different voltages. At higher voltages, the cavity shifts to a lower wavelength, owing to the free carrier injection in GaAs.

The quantum confined Stark shift is observed by monitoring the resonance of a QD as shown in figure 8(b). Even without applying a voltage, built-in potential is present in the p–i–n diode. When forward bias is applied, the electric field across the QD decreases, and a blue shift
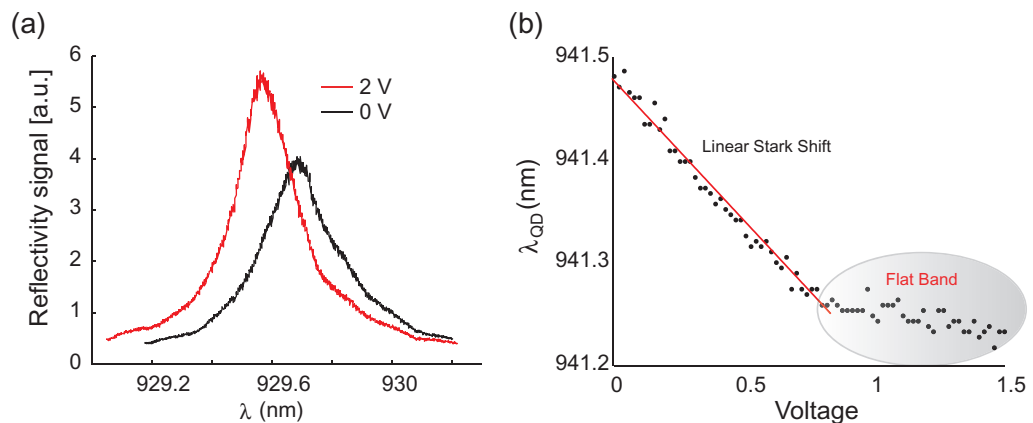
Figure 8. (a) Blue shift of the cavity resonance (probed in reflectivity) as voltage is applied across the p–i–n junction. (b) Stark shift of a QD as a function of applied voltage.

is observed. The shift is linear, owing to the large permanent dipole moment of the dot along the vertical direction. However, at large forward bias, the flatband is reached, and the QD frequency no longer shifts. A larger Stark shift could be observed when a reverse bias is applied to the QD, as a reverse bias increases the electric field across the QD. However, in our system the electron and hole pair tunnels out of the dot in reverse bias and the photoluminescence is quenched.

The vertical electrical control is relevant not only for controlling the QD resonance frequency but also for deterministic loading of QDs with electrons or holes [30]. It has been shown that the spin states of charged excitons can be completely controlled using fast laser pulses [5, 6], and the next step is to extend this type of experiments for QDs coupled to resonators.

In addition to electro-optic switching, all-optical switching at the single-photon level is also possible to be implemented using a single cavity–QD system. This can be implemented either by using saturation nonlinearities [4], as demonstrated for a cavity probed in reflectivity in [15], or by using quantum nonlinearities and operating in the photon blockade or photon-induced tunneling regime. To ensure the practicality of these types of devices, it is desirable for the nonlinear medium consisting of the cavity and the QD to be connected to multiple waveguides that channel the signal and the control light fields, as shown in figure 9. The device consists of a linear three-hole defect cavity coupled to three waveguides, one aligned to the cavity (x-direction in figure 9) and two others that make a $\pi/3$ angle with the cavity axis [31]. Each waveguide is terminated with a grating coupler that allows coupling from a direction perpendicular to the chip plane such that the device can be probed from the top using a confocal microscope setup [32].

4. Conclusion

The devices presented in this paper are representative of the very recent developments in integrated quantum photonic technologies on photonic crystal chips. These types of structures are essential for implementing the devices used in information processing at the classical and the quantum level. An essential next step in this direction is to build reliable networks of single
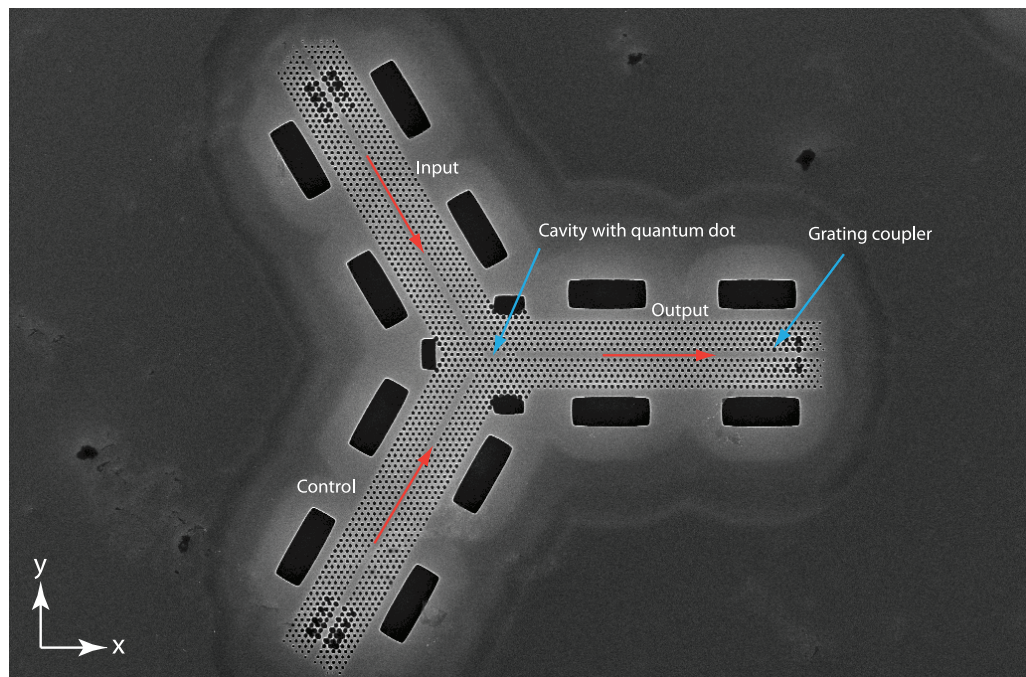
Figure 9. The photonic crystal network integrating three waveguides coupled to a single photonic crystal cavity. This device could be used for all-optical switching where the signal and control beams come from different ports on the chip.

emitters coupled to resonators interconnected via photonic waveguides. These types of devices will help to develop the experimental knowledge for efficiently controlling and routing light pulses of low photon number. This kind of control will enable classical optical signal processing devices to operate at the ultralow power level. For quantum information processing, it is first required to achieve coherent control of the quantum states for QD spin states (electron or hole) in a cavity [5, 6]. On-chip integration will then be required in order to entangle distant quantum emitters on the chip and to implement quantum repeaters [33] and simulators based on a relatively small number (tens) of quantum nodes [34].

Acknowledgments

References

[1] O'Brien J L, Furusawa A and Vuckovic J 2009 Photonic quantum technologies *Nat. Photonics* **3** 687–95
[2] Nielsen M A and Chuang I L 2000 *Quantum Computation and Quantum Information* (Cambridge: Cambridge University Press)
[3] Michler P 2003 *Single Quantum Dots: Fundamentals, Applications and New Concepts* (*Topics in Applied Physics*) (Berlin: Springer) **90**

[4] Englund D, Faraon A, Fushman I, Stoltz N, Petroff P and Vuckovic J 2007 Controlling cavity reflectivity with a single quantum dot *Nature* **450** 857–61

[5] Press D, Ladd T D, Zhang B and Yamamoto Y 2008 Complete quantum control of a single quantum dot spin using ultrafast optical pulses *Nature* **456** 218–21

[6] Kim E D, Truex K, Xu X, Sun B, Steel D G, Bracker A S, Gammon D and Sham L J 2010 Fast spin rotations by optically controlled geometric phases in a charge-tunable InAs quantum dot *Phys. Rev. Lett.* **104** 167401

[7] Vahala K 2003 Optical microcavities *Nature* **424** 839–46

[8] Noda S, Chutinan A and Imada M 2000 Trapping and emission of photons by a single defect in a photonic bandgap structure *Nature* **407** 608–10

[9] Noda S 2006 Recent Progresses and future prospects of two- and three-dimensional photonic crystals *J. Lightw. Technol.* **24** 4554–67

[10] Akahane Y, Asano T, Song B-S and Noda S 2003 High-*Q* photonic nanocavity in a two-dimensional photonic crystal *Nature* **425** 944–7

[11] Hennessy K, Badolato A, Winger M, Gerace D, Atatüre M, Gulde S, Falt S, Hu E and Imamoglu A 2007 Quantum nature of a strongly coupled single quantum dot–cavity system *Nature* **445** 896–9

[12] Yoshie T, Scherer A, Hendrickson J, Khitrova G, Gibbs H M, Rupper G, Ell C, Shchekin O B and Deppe D G 2004 Vacuum Rabi splitting with a single quantum dot in a photonic crystal nanocavity *Nature* **432** 200–3

[13] Waks E and Vučković J 2006 Dipole induced transparency in drop-filter cavity–waveguide systems *Phys. Rev. Lett.* **93** 153601

[14] Faraon A, Majumdar A, Kim H, Petroff P and Vuckovic J 2010 Fast electrical control of a quantum dot strongly coupled to a nano-resonator *Phys. Rev. Lett.* **104** 047402

[15] Fushman I, Englund D, Faraon A, Stoltz N, Petroff P and Vuckovic J 2008 Controlled phase shifts with a single quantum dot *Science* **320** 769–72

[16] Imamoglu A, Schmidt H, Woods G and Deutsch M 1997 Strongly interacting photons in a nonlinear cavity *Phys. Rev. Lett.* **79** 1467–70

[17] Birnbaum K M, Boca A, Miller R, Boozer A D, Northup T E and Kimble H J 2005 Photon blockade in an optical cavity with one trapped atom *Nature* **436** 87–90

[18] Faraon A, Fushman I, Englund D, Stoltz N, Petroff P and Vuckovic J 2008 Coherent generation of non-classical light on a chip via photon-induced tunnelling and blockade *Nat. Phys.* **4** 859–63

[19] Kimble H J 2008 The quantum internet *Nature* **453** 1023–30

[20] Schneider C, Strauss M, Sunner T, Huggenberger A, Wiener D, Reitzenstein S, Kamp M, Hofling S and Forchel A 2008 Lithographic alignment to site-controlled quantum dots for device integration *Appl. Phys. Lett.* **92** 183101

[21] Faraon A, Englund D, Fushman I, Stoltz N, Petroff P and Vuckovic J 2007 Local quantum dot tuning on photonic crystal chips *Appl. Phys. Lett.* **90** 213110

[22] Faraon A, Englund D, Bulla D, Luther-Davies B, Eggleton B J, Stoltz N, Petroff P and Vuckovic J 2008 Local tuning of photonic crystal cavities using chalcogenide glasses *Appl. Phys. Lett.* **92** 043123

[23] Faraon A and Vuckovic J 2009 Local temperature control of photonic crystal devices via micron-scale electrical heaters *Appl. Phys. Lett.* **95** 043102

[24] Hennessy K, Högerle C, Hu E, Badolato A and Imamoglu A 2006 Tuning photonic nanocavities by atomic force microscope nano-oxidation *Appl. Phys. Lett.* **89** 041118

[25] Seo M-K, Park H-G, Yang J-K, Kim J-Y, Kim S-H and Lee Y-H 2008 Controlled sub-nanometer tuning of photonic crystal resonator by carbonaceous nano-dots *Opt. Express* **16** 9829–47

[26] Faraon A, Fushman I, Englund D, Stoltz N, Petroff P and Vuckovic J 2008 Dipole induced transparency in waveguide coupled photonic crystal cavities *Opt. Express* **16** 12154–62

[27] Devitt S J, Greentree A D, Ionicioiu R, O'Brien J L, Munro W J and Hollenberg L C L 2007 Photonic module: an on-demand resource for photonic entanglement *Phys. Rev.* A **76** 052312

[28] Högele A, Seidl S, Kroner M, Karrai K, Warburton R J, Gerardot B D and Petroff P M 2004 Voltage-controlled optics of a quantum dot *Phys. Rev. Lett.* **93** 217401

IOP Institute of Physics ◆ DEUTSCHE PHYSIKALISCHE GESELLSCHAFT

[29] Hofbauer F, Grimminger S, Angele J, Bohm G, Meyer R, Amann M C and Finley J J 2007 Electrically probing photonic bandgap phenomena in contacted defect nanocavities *Appl. Phys. Lett.* **91** 201111

[30] Medeiros-Ribeiro G, Leonard D and Petroff P M 1995 Electron and hole energy levels in InAs self-assembled quantum dots *Appl. Phys. Lett.* **66** 1767–9

[31] Faraon A, Waks E, Englund D, Fushman I and Vuckovic J 2007 Efficient photonic crystal cavity–waveguide couplers *Appl. Phys. Lett.* **90** 073102

[32] Englund D, Ellis B, Edwards E, Sarmiento T, Harris J S, Miller D A B and Vuckovic J 2009 Electrically controlled modulation in a photonic crystal nanocavity *Opt. Express* **17** 15409–19

[33] Childress L, Taylor J M, Sørensen A S and Lukin M D 2005 Fault-tolerant quantum repeaters with minimal physical resources and implementations based on single-photon emitters *Phys. Rev.* A **72** 052330

[34] Buluta I and Nori F 2009 Quantum simulators *Science* **326** 108–11